

© 2016. This manuscript version is made available under the CC-BY-NC-ND 4.0 license  
<http://creativecommons.org/licenses/by-nc-nd/4.0>

# Anion Photoelectron Spectroscopy and CCSD(T) Calculations of the $\text{Cl}^- \cdots \text{N}_2$ Complex

Peter D. Watson<sup>a</sup>, Hai-wang Yong<sup>b</sup>, Kim M. L. Lapere<sup>a</sup>, Marcus Kettner<sup>a</sup>, Allan J. McKinley<sup>a</sup>, Duncan A. Wild<sup>a,\*</sup>

<sup>a</sup>*School of Chemistry and Biochemistry The University of Western Australia, Crawley, Western Australia, 6009*

<sup>b</sup>*School of Physical Sciences University of Science and Technology of China, Jinzhai Road 96, Hefei 230026, Anhui Province, P.R. China*

---

## Abstract

The gas phase anion photoelectron spectrum of the  $\text{Cl}^- \cdots \text{N}_2$  complex is presented, allowing determination of the electron binding energy, and is compared to CCSD(T) calculations. The calculations reveal three stationary points on the neutral complex surface; a linear  $C_{\infty v}$  and two  $C_{2v}$  symmetry geometries. For the anion complex, two geometries are predicted, similar to the  $C_{2v}$  symmetry conformations determined for the neutral. Comparing both computational and experimental results with those from previous work we show trends between anion complex stability and electron stabilisation energy and also the neutral complex stability with respect to the polarisability of the halogen

*Keywords:* Spectroscopy, gas phase anions, photoelectron, mass spectrometry

---

## 1. Introduction

Anion photoelectron spectroscopy offers an avenue by which to investigate the electronic structure of transient species in the gas phase by accessing the neutral states via a stable anion analogue. When coupled with mass spectrometric techniques, the separation of ion-molecule complexes in a gas mixture allows for only the complex of interest to be scrutinised. The appreciable power of this technique is apparent from numerous examples in literature, for example in references [1–4].

The impact of chlorine and other halide-containing molecules in gas phase interactions has been explored extensively in recent decades. Initially interest was spurred on by the impact that commercial chlorofluorocarbons (CFCs) proved to have on the depletion of stratospheric ozone [5]. However given the complexity of atmospheric chemistry, the contribution of other species in a range of reactions was also explored, with some representative examples given in References[6–10]. Nitrogen, as the most abundant gas in Earth’s atmosphere, would serve as an ideal point of interest as it is able to mediate many atmospheric reactions by solvating clusters in the gas phase[7, 11]. The example given in reactions 1a and 1b shows nitrogen acting as a cluster partner to an  $\text{NO}^+$  ion and is “switched” for a water molecule going on to produce  $\text{HNO}_2$ .



Under atmospheric conditions (in this case in the D layer), the direct addition of water to  $\text{NO}^+$  is too slow to account for its atmospheric abundance and as such complexation by nitrogen is suggested to provide more favourable pathways for such systems. Yet there is surprisingly few studies completed on nitrogen-containing clusters, perhaps due to its high stability and tendency to act only indirectly or as a precursor to more reactive species such as  $\text{NO}_x$ .

Other than in our own atmosphere, halide-nitrogen complexes may well exist on extraterrestrial bodies which hold a significant nitrogen abundance. Considering only our own solar system, we find four prominent examples in Venus, Pluto, Titan and Triton. Taking Pluto, the ice covering its surface is predicted from infrared reflectance spectroscopy to be approximately 98% nitrogen with atmospheric pressures of 3mbar at the surface[11]. Recent passes by the New Horizons probe has shown that due to Pluto’s lack of a magnetic field and small escape velocity ( $0.95 \text{ km s}^{-1}$ )[11] the exposure of the atmosphere to solar winds sweeps this atmosphere out into a tail much like a comet[12]. This tail, and indeed other comet tails could be representative of a highly charged environment and present the possibility of the formation of ion-molecule complexes through both direct[13] and dissociative electron attachment[14].

There is a conspicuous paucity of prior work in the literature in the area of halide-nitrogen complexes and their potential impact in both our atmosphere and extraterrestrially, in particular research done experimentally. We wish to expand on previously published spectroscopic and computational studies undertaken in the Wild group on the bromide and iodide complexes with nitrogen[15] by attending to the chloride species in the present work. This would

---

\*Corresponding author

Email address: [duncan.wild@uwa.edu.au](mailto:duncan.wild@uwa.edu.au) (Duncan A. Wild)

bring us closer to completing the suite of halide-nitrogen complexes studied.

There have been three studies on weakly bound halide-nitrogen complexes; one by Matsubara and Hiraoka[16], another by Hiraoka[17] and previously noted, work by the Wild group regarding  $\text{Br}^- \cdots \text{N}_2$  and  $\text{I}^- \cdots \text{N}_2$  clusters[15]. Hiraoka performed MP2 calculations on these anionic fluoride complexes with  $\text{O}_2$ ,  $\text{N}_2$  and  $\text{CO}$  molecules using 6-311+G\*\* and 3-21G\* basis sets on the  $\text{F}^-$  ion and  $\text{N}_2$  respectively, reporting that the singly-bound complex is of  $C_{2v}$  symmetry and the doubly-bound complex is  $D_{2h}$ . However, Matsubara performed calculations on the clusters formed between  $\text{H}^-$ ,  $\text{Li}^-$  and  $\text{F}^-$  with a variety of diatomic molecules including nitrogen, using B3LYP and 6-311++G\*\* basis sets. Matsubara reports structures of the singly-bound fluoride-nitrogen complex to be  $C_s$  symmetry and  $C_{2v}$  and then  $C_{2h}$  symmetry for the  $\text{F}^- \cdots (\text{N}_2)_2$  complex. A comparison of the geometric structures of the two singly bound complexes as presented by Matsubara and Hiraoka is given in Table 1 (Hiraoka’s results seem more appropriate as the B3LYP functional without empirical corrections does not account for longer range dispersion interaction as is present in the cases of van der Waals (vdW) complexes[18]).

Table 1: Comparison between calculated geometries from Matsubara[16] and Hiraoka[17]

	Point Group	$r_{\text{X}\cdots\text{   }}^*$ [Å]	$r_{\text{N}\equiv\text{N}}$ [Å]	$\angle_{\text{X}\cdots\text{   }-\text{N}}$ [°]
Matsubara[16]	$C_s$	2.722	1.104	60.9
Hiraoka[17]	$C_{2v}$	2.917	1.12	90.0

\* ||| is the mid point of the  $\text{N}\equiv\text{N}$  bond

## 2. Methodology

### 2.1. Experimental Methods

All experiments were conducted using a time of flight mass spectrometer coupled to a magnetic bottle photoelectron spectrometer (TOF-PES) based on designs from both Cheshnovsky[19] and Wiley and McLaren[20]. Extensive detail of the apparatus is given in the seminal references above and also in previous publications from the Wild group[21–23]. The gas mixture prepared for these experiments consisted of a halogen source (in this case trace amounts of  $\text{CCl}_4$  vapour) along with nitrogen gas with a partial pressure of 40 kPa then backed to the operational pressure of 450 kPa with argon gas. This gas mixture is injected into the TOF-PES via a pulsed solenoid valve and intersected with a beam of electrons to produce anion complexes which drift towards the ion flight tube. Often residual halide sources from previous experiments are part of this gas mix, however they prove beneficial in the calibration of recorded mass spectra and mass separation is sufficient to interrogate only the desired complexes.

Complexes are intersected with a 5 ns pulse of 266 nm radiation (4.66 eV), being the fourth harmonic of a Nd:YAG laser (Spectra Physics Quanta Ray Pro) to detach photoelectrons which are collected by the magnetic bottle[19]. Photoelectrons are detected by a microchannel plate (MCP) detector at the end of a 1.8 m photoelectron flight tube. To improve detection efficiency, a grounded mesh sits 2 cm in front of the detector and the front plate of MCP is positively biased (200 V). By determining the electron kinetic energy ( $e\text{KE}$ ) from the time of flight of the photoelectrons, the electron binding energy ( $e\text{BE}$ ) for the transition they are associated with can be determined via the following equation:

$$e\text{BE} = h\nu - e\text{KE} \quad (2)$$

where  $h\nu$  is the energy carried by the 266 nm photon. Spectra are built up as a histogram of photoelectron counts over 10000 laser pulses, which are calibrated, averaged and smoothed over the course of experimentation.

After calibration the intensities in a spectrum undergo a Jacobi transform (multiply by  $t^3$ ) such that they are with respect to energy rather than time. The Jacobi transform adds to the symmetry of peaks by increasing their tails (ie. larger values of  $t$ ), however as the binding energy approaches that of the laser (4.66 eV), the long electron flight time leads to a significant increase in the intensity of the background signal.

In the calibration of these experiments, the separation of the  $^2P_{3/2}$  and the  $^2P_{1/2}$  states of the bare chloride is less than the resolution of the spectrometer, thus making them difficult to distinguish accurately. As such only spectra recorded of the bromide ion is used to calibrate the chloride complex spectra and the peak positions in these spectra are reported as corresponding to the  $^2P_{3/2}$  transition as this state will feature more dominantly.

Finally, the spread in electron energies ( $dE_e$ ) of the magnetic bottle photoelectron spectrometer depends on the ion mass and kinetic energy. According to Chenovsky et al[19],  $dE_e$  is given by,

$$dE_e = 4\sqrt{\frac{m_e}{m_I} E_e E_I} \quad (3)$$

where  $m_e$ ,  $m_I$ ,  $E_e$ , and  $E_I$  are the masses and kinetic energies of the detached electron and anion. The ions have approximately 1000 eV of kinetic energy, and hence for an electron with kinetic of energy 1.05 eV, i.e., detached from the chloride ion following absorption of 4.66 eV radiation, the spread in energies is therefore 0.52 eV leading to a resolution of 0.21 eV (full width half maximum, FWHM).

### 2.2. Computational Methods

Ab initio calculations were performed at the CCSD(T) level of theory for the chloride-nitrogen complexes using the Gaussian 09 software package[24]. Augmented correlation consistent basis sets developed by Dunning[25, 26] were employed for both nitrogen and chlorine (aug-cc-pVnZ  $n = \text{T, Q, 5}$  representing the triple, quadruple and

quintuple- $\zeta$  basis sets with chlorine including additional diffuse functions). Energies of the bare halogen anions and neutrals are calculated along with the nitrogen molecule to later compare with complex energies and calculate values of the cluster binding energy  $D_e$  and true cluster binding energy  $D_0$ . Complex geometries were optimised using the triple- $\zeta$  basis sets with strict convergence criteria ( $1 \times 10^{-8} E_h a_0^{-1}$ ) due to the expected loosely bound nature of such systems. Each optimisation was followed by vibrational frequency analysis of these geometries. The complete basis set limit energy was produced by extrapolation through quadruple- $\zeta$  and quintuple- $\zeta$  single point energies using the two point extrapolation scheme given in equation 4, where  $\alpha = 5$  for SCF extrapolation and  $\alpha = 3$  for CCSD(T) correlation energy extrapolation,  $E(L)$  is the energy resulting from a certain basis set,  $A$  is a parameter and  $E_\infty$  is the energy of the complete basis set[15].

$$E(L) = E_\infty + \frac{A}{L^\alpha} \quad (4)$$

Comparison is also made between previously calculated energies at MP2 for the chloride-nitrogen complex and between other halide-nitrogen complexes at both MP2 and CCSD(T) levels of theory.

### 3. Results and discussion

#### 3.1. Computational Results

Rudimentary electrostatic modelling of the halide- $N_2$  complexes has been completed previously, with the multipole expansion taking into account charge-quadrupole and charge-hexadecapole electrostatic interactions and the charge-induced dipole interaction (equation 5)[15].

$$V_{\text{elec}}(R, \theta) = \frac{q}{4\pi\epsilon_0} \left( \frac{\Theta(3 \cos^2 \theta - 1)}{2R^3} + \frac{\Phi(35 \cos^4 \theta - 30 \cos^2 \theta + 3)}{8R^5} \right)$$

$$V_{\text{ind}}(R, \theta) = -\frac{q^2(\alpha_{\parallel} \cos^2 \theta + \alpha_{\perp} \sin^2 \theta)}{2(4\pi\epsilon_0)^2 R^4} \quad (5)$$

As in a previous publication[15] the values are  $\Theta = -4.994 \times 10^{-40} \text{ C m}^2$  and  $\Phi = -8.493 \times 10^{-60} \text{ C m}^4$  for the quadrupole and hexadecapole moments respectively and  $\alpha_{\parallel} = 2.436 \times 10^{-40} \text{ C}^2 \text{ m}^2 \text{ J}^{-1}$  and  $\alpha_{\perp} = 1.670 \times 10^{-40} \text{ C}^2 \text{ m}^2 \text{ J}^{-1}$  for the parallel and perpendicular dipole polarisabilities of the nitrogen molecule [27].

The electrostatic model of the halide-nitrogen complexes treat the halide as a point charge as well as omitting the hard wall repulsion present and hence fails to accurately describe the impact the halide size has on the interaction. That being said, the model suggests that the anion complexes should exhibit a T-shaped structure which is due to the dominance of the charge-quadrupole interaction

despite the anisotropy in the polarisabilities of the nitrogen molecule ( $\alpha_{\parallel} > \alpha_{\perp}$ ) which favours a linear complex considering only the charge-induced dipole interaction. The anisotropy would suggest that the neutral complex would have a linear geometry, being dominated by dispersion interactions.

#### 3.1.1. CCSD(T) Calculations

We begin our analysis of the results of the CCSD(T) calculations by focussing on the neutral species, with a complete data set provided in Supplementary Information. Geometry optimisation calculations predicted three stationary points on the neutral surface with data presented in Table 2. The geometries correspond to a  $C_{\infty v}$  and two  $C_{2v}$  symmetry conformations, with one of the two  $C_{2v}$  geometries showing much shorter distances between the chlorine and nitrogen atoms (almost half) and the N–N bond length increasing from 1.104 Å to 1.290 Å. This increased bond length more closely resembles a double bond similar to that of molecular oxygen (1.213 Å). Accordingly, in a subsequent vibrational analysis, the harmonic frequencies are significantly higher than what one would expect from loosely bound vdW complexes for the vibrational modes assigned to the Cl–N–N bend and Cl $\cdots$ N stretch and lower in energy for the N–N stretch. Through a Roby analysis (completed using Tonto[28]) it is shown that the Cl–N bond in this structure is at least 92% covalent suggesting that this conformation is a more tightly bound triangular complex (referred to as “Tri”)[23].

Table 2: Geometrical parameters of the chlorine- $N_2$  gas phase neutral complexes from CCSD(T) calculations.  $D_e$  values are derived from CCSD(T)/CBS results, while  $D_0$  utilises the CCSD(T)/aug-cc-PVTZ computed harmonic zero point energies.

	$r_{X\cdots   }^*$ [Å]	$r_{X-N}$ [Å]	$r_{N\equiv N}$ [Å]	$\angle_{X-N-N}$	$D_e$ [kJ mol $^{-1}$ ]	$D_0$ [kJ mol $^{-1}$ ]
Tee	3.513	3.556	1.104	81.1°	1.3	1.1
Tri	1.735	1.851	1.290	69.6°		
Lin	3.741	3.189	1.104	180.0°	3.5	2.7
$N_2$			1.104			

\* ||| is the mid point of the N $\equiv$ N bond

Table 3: Geometrical parameters of the  $C_{2v}$  chloride- $N_2$  gas phase anion complexes from CCSD(T) calculations.  $D_e$  values are derived from CCSD(T)/CBS results, while  $D_0$  utilises the CCSD(T)/aug-cc-PVTZ computed harmonic zero point energies.

	$r_{X\cdots   }^*$ [Å]	$r_{X-N}$ [Å]	$r_{N\equiv N}$ [Å]	$\angle_{X-N-N}$	$D_e$ [kJ mol $^{-1}$ ]	$D_0$ [kJ mol $^{-1}$ ]
Tee	3.544	3.587	1.104	81.2°	9.3	8.5
Tri	1.686	1.839	1.468	66.5°		
$N_2$			1.104			

\* ||| is the mid point of the N $\equiv$ N bond

The other  $C_{2v}$  complex (referred to as “Tee”) exhibits a geometry consistent with a vdW type complex. The N–N bond length in the complex remains unchanged from the nitrogen molecule and the X–N separation is 3.556 Å.

However, considering the vibrational frequency analysis this complex displays an imaginary frequency corresponding to the X–N–N bending mode suggesting it is a transition state. The linear complex lies  $1.6 \text{ kJ mol}^{-1}$  below this geometry (energies are extrapolated to the complete basis set and include zero point energies from the triple- $\zeta$  harmonic vibrational analysis). The linear complex displays all real frequencies. The CCSD(T) calculations indicate that the linear complex is the most stable geometry for the neutral complex, although the complex dissociation energies in both the linear and “Tee” geometries are small which results from the interaction being only inductive.

Considering the anion potential energy surfaces now we note the lack of a stationary point corresponding to the linear geometry, not unexpected if we again use the electrostatic model as a guide. We find two stationary points of  $C_{2v}$  symmetry (given in Table 3) which are the anion analogues of the neutral “Tri” and “Tee” complexes as Cl–N separations for these complexes are  $1.839 \text{ \AA}$  and  $3.587 \text{ \AA}$  respectively. As for the neutral complexes the anion “Tri” complex lies much higher in energy compared to the global minimum ( $847.1 \text{ kJ mol}^{-1}$  for the anion and  $466.0 \text{ kJ mol}^{-1}$  for the neutral). With this in mind the stable conformation of the anion complex is the “Tee” complex and upon electron detachment the corresponding neutral complex would vibrationally cool to adopt the linear geometry.

### 3.1.2. Electron Detachment Energies

Electron detachment energies for the complexes are determined from CCSD(T) calculations to be later compared with experimental results. Calculations for the chlorine atom give an electron detachment energy at the complete basis set for the bare halide. The spin-orbit coupling constant of the bare halide is determined using the experimentally known separation of the  $^2P$  states of chlorine and applied to the calculated electron detachment energies. Comparison with experimental energy levels yields a correction to account for shortcomings in the calculations, this is then applied to all subsequent calculated transitions[29]. In the case of chlorine the determined shifts for the quintuple- $\zeta$  and complete basis sets were  $0.016 \text{ eV}$  and  $-0.015 \text{ eV}$  respectively suggesting that both these basis sets are appropriate for these kind of calculations considering the resolution of the TOF-PES is  $0.21 \text{ eV}$ .

The calculated adiabatic electron detachment energy (ADE) for the chloride-nitrogen complex is  $3.67$  and  $3.78 \text{ eV}$  for the  $^2P_{3/2}$  and  $^2P_{1/2}$  states respectively, while the predicted vertical detachment energies (VDE) are  $3.69$  and  $3.80 \text{ eV}$  to the two states. Further discussion of these results with respect to experiment and with other halide-nitrogen complexes follows. However at this point it is worth noting the spin-orbit splitting present in the chloride species is small ( $0.109 \text{ eV}$ [30]) and it may prove difficult to separate the two  $^2P$  states in experiment due to the resolution of the TOF-PES.

## 3.2. Experimental Results

### 3.2.1. Mass Spectrometry

A representative mass spectrum for the  $\text{N}_2\text{-Ar-CCl}_4$  gas mix is presented in Figure 1. Clear signals are observed for both isotopes of chlorine and bromine, allowing for calibration of the remaining peaks in the spectrum. The peaks at 63 and 65 amu correspond to the  $^{35}\text{Cl}^- \dots \text{N}_2$  and  $^{37}\text{Cl}^- \dots \text{N}_2$  complexes respectively. These are easily identifiable as chlorine peaks due to the ratio of the signal intensity corresponding closely to the isotopic ratio for  $^{35}\text{Cl}$  and  $^{37}\text{Cl}$ .

Other peaks in the spectrum are observed at 53 and 55, 71 and 73 and 75 and 77 amu which are from the isotope pairs of the chloride-water, chloride-oxygen and the chloride-argon complexes. Peak positions at 79 and 81 amu correspond to the bromide isotope pair and are the result of previous experiments’ bromide halide source adsorbing to the interior of the gas mixing station. The spectrum does not show further degrees of solvation by nitrogen as the signal intensity typically decreases rapidly with further coordination. No significant signal for the larger clusters was found during experiment which highlights the difficulty in producing these kind of transient complexes in the gas phase.

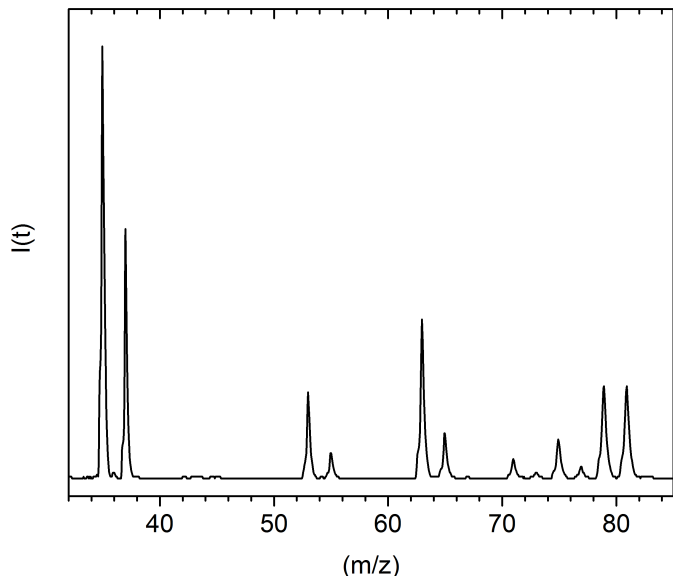


Figure 1: Mass spectrum of the  $\text{N}_2\text{-Ar-CCl}_4$  gas mix

### 3.2.2. Photoelectron Spectroscopy Results

Photoelectron spectra of the chloride and bromide ions were recorded for calibration purposes however as expected the lower resolution of the TOF-PES meant that peaks corresponding to transitions to the  $^2P$  states of the chlorine could not be separated and only the bromide ion spectrum was used for calibration. The recorded spectrum of  $\text{Cl}^- \dots \text{N}_2$  was then processed, first by calibration and then a Jacobi transform on the intensities, followed by smoothing.

The spectrum is presented in Figure 2 over the range of electron binding energy from 0.00 to 4.66 eV, and features a single band, with a maximum at 3.75 eV. At higher electron binding energy (4.00 to 4.66 eV) the evidence of the Jacobi transform’s influence on background noise is readily apparent. The spectrum is truncated at 4.66 eV as this is the highest energy possible in the spectrum.

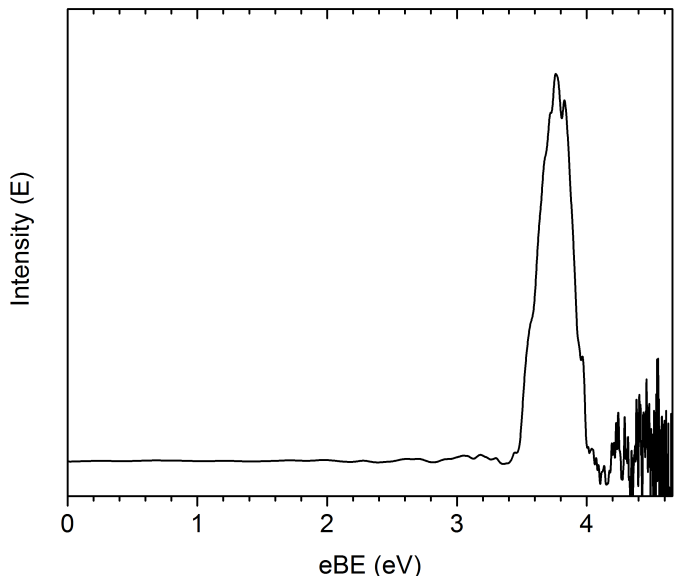


Figure 2: Photoelectron spectrum of the chloride-nitrogen complex

A fitting procedure was applied to the spectral feature assuming that it is composed of two closely spaced transitions from the anion to the neutral  ${}^2P_{3/2}$  and  ${}^2P_{1/2}$  spin orbit states which, due to the spectral resolution being 0.21 eV, are unresolved. The transition to each state was modelled as a Gaussian profile with FWHM initially defined by the instrument resolution. The separation of the two Gaussians (i.e., the spin orbit splitting of the chlorine  ${}^2P$  states, being 0.109 eV [30]), and the intensity ratio of 2:1 (arising from the state degeneracy for  $J = 3/2$  and  $1/2$ ) were held constant during the fitting procedure.

The fit to the experimental band is provided in Figure 3 (red curve), with the two component Gaussian functions (blue and green curves). The fit provides an estimate for the VDEs to the  ${}^2P_{3/2}$  and  ${}^2P_{1/2}$  states as 3.72 and 3.83 eV respectively. There is good agreement between the experimentally determined and predicted VDE. Prior to correction for spin-orbit splitting and shifting correction, the calculated VDE is 3.74 eV. After taking into account the correction factors, the predicted VDE to be 3.69 and 3.80 eV. Further corrections could be applied to the calculated results to account for the perturbation of the halogen spin orbit state separation by the coordinated nitrogen, however considering the calculated complex dissociation energy of the neutral the degree of perturbation is expected to be negligible. The predicted VDE values lie within 0.03 eV of the values estimated from the fit to the experimental band.

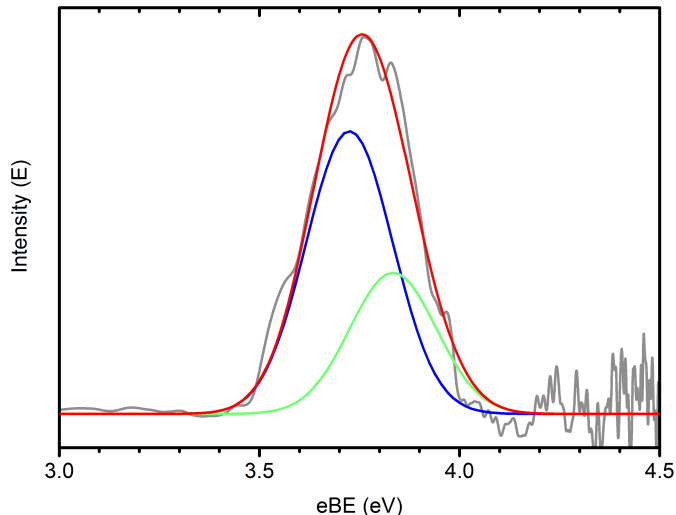


Figure 3: Fit of the experimental band to the sum of two gaussian functions. Blue is the transition to the  ${}^2P_{3/2}$  state, Green is the transition to the  ${}^2P_{1/2}$  state, and Red is the sum of the two

### 3.3. Comparison with other halide-nitrogen complexes

Previous work [15] provided both experimental and CCSD(T) results for the analogous bromide and iodide complexes and some information on the fluoride-nitrogen complex. These are presented alongside the current data here in Table 4. For the singularly coordinated complexes we are able to identify several trends.

Table 4: Comparison between halide-nitrogen complexes[15, 23]

	$P_{3/2}$ (eV)	$P_{1/2}$ (eV)	$E_{stab}$ (meV)	$D_o$ anion (kJ mol $^{-1}$ )	$D_o$ neutral (kJ mol $^{-1}$ )
FN $_2$	—	—	—	15.7	—
ClN $_2$	3.72	3.83	110	8.5	1.1
BrN $_2$	3.43	3.92	40	7.8	1.8
IN $_2$	3.07	4.02	20	7.0	2.4

From our experimental data the electron stabilisation energy ( $E_{stab}$ ), i.e., the difference between the energies of the transitions to the  ${}^2P_{3/2}$  state in the bare halide and in the complexes, is calculated. We can see that there is a moderate linear correlation between the anion complex stabilisation energy ( $D_0$ ) and the complex electron stabilisation energy ( $E_{stab}$ ). We can also see that the complex dissociation energy (for the ‘Tri’ complexes) decreases as you move through the halide series, appearing to adhere to periodic trends. This is associated with the nature of the halide as an electron donor, fluoride on one hand is much smaller and a ‘harder’ Lewis acid, whereas iodide is ‘softer’ and more diffuse. On the other hand the values of  $D_0$  in the neutral complexes increase on moving through the halide series (Cl $\cdots$ N $_2$  to I $\cdots$ N $_2$ ). They are much lower than the  $D_0$  values of the anion series. Both of these observations are due to the nature of the interaction binding the complexes. In the anions, as electrostatic models

have suggested, the charge-quadrupole interaction is dominant and would result in stronger interaction, whereas in the neutral species it is only dispersion forces binding the complexes. This suggests that firstly; the interaction is much weaker, and secondly; that the polarisability of the halide determines the strength of interaction. With this in mind it is not surprising that the iodine complex is the most strongly bound having the largest polarisability while the chlorine complex features the weakest intermolecular interaction.

#### 4. Summary

Ab initio calculations have also been performed on the chloride-nitrogen complex as well as the neutral analogue at CCSD(T) level of theory. We report the vertical detachment energy (VDE) and therefore the electron affinity of the neutral as 3.72 eV which shows good agreement with calculated values of 3.69 eV and 3.80 eV for the two  $^2P$  states when considering the resolution of the TOF-PES apparatus.

CCSD(T) calculations predict five stationary points, three for the neutral and two for the anion complexes. A linear structure, present only in the neutral, a pair of geometries of  $C_{2v}$  symmetry but with comparably shorter bond lengths than the linear and two other  $C_{2v}$  conformations that are much more weakly bound and typical of van der Waals complexes. The linear complex is suggested to be the most favourable form of the neutral complex while the  $C_{2v}$  van der Waals complex is the most stable form of the anion.

Comparison is also made here between the chloride-nitrogen complex and other halide-nitrogen complexes studied previously. We note a correlation between the experimental electron binding energy ( $^2P_{3/2}$ ) and the calculated complex dissociation energies for the anion. This trend can be rationalised by the strength of the halide ions as Lewis donors. In the neutrals the  $D_0$  values increase from chlorine to iodine which can be associated with the increase in the polarisability of the halogen atoms as atomic size increases.

#### 5. Acknowledgements

KLM and MK acknowledge the support of an Australian Postgraduate Award (APA). HY acknowledges the support of the UWA - China Research Training Program. We acknowledge financial support from the Faculty of Science and the School of Chemistry and Biochemistry, and the Australian Research Council is acknowledged for funding the laser installation under the LIEF scheme (LE110100093).

#### 6. References

- [1] U. Boesl, W. J. Knott, Negative ions, mass selection, and photoelectrons, *Mass Spectrometry Reviews* 17 (4) (1998) 275–305. doi:10.1002/(SICI)1098-2787(1998).
- [2] T. Lenzer, M. R. Furlanetto, K. R. Asmis, D. M. Neumark, Zero electron kinetic energy and photoelectron spectroscopy of the  $\text{XeI}^-$  anion, *The Journal of Chemical Physics* 109 (24) (1998) 10754–10766. doi:10.1063/1.477774.
- [3] X. Li, L.-S. Wang, Probing the electronic structure of mono-nitrogen doped aluminum clusters using anion photoelectron spectroscopy, *The European Physical Journal D* 34 (1-3) (2005) 9–14. doi:10.1140/epjd/e2005-00100-3.
- [4] B. Opoku-Agyeman, A. S. Case, J. H. Lehman, W. C. Lineberger, A. B. McCoy, Nonadiabatic photofragmentation dynamics of  $\text{BrCN}^-$ , *J. Chem. Phys.* 141 (8) (2014) 084305. doi:10.1063/1.4892981.
- [5] M. J. Molina, F. S. Rowland, Stratospheric sink for chlorofluoromethanes: chlorine atom-catalysed destruction of ozone, *Nature* 249 (5460) (1974) 810–812. doi:10.1038/249810a0.
- [6] R. R. Garcia, S. Solomon, A new numerical model of the middle atmosphere: 2. ozone and related species, *Journal of Geophysical Research* 99 (D6) (1994) 12937–12951. doi:10.1029/94jd00725.
- [7] E. E. Ferguson, F. Arnold, Ion chemistry of the stratosphere, *Accounts of Chemical Research* 14 (11) (1981) 327–334. doi:10.1021/ar00071a001.
- [8] M. Bartolomei, E. Carmona-Novillo, M. I. Hernandez, J. Campos-Martinez, R. Hernandez-Lamoneda, Long-range interaction for dimers of atmospheric interest: dispersion, induction and electrostatic contributions for  $\text{O}_2\text{-O}_2$ ,  $\text{N}_2\text{-N}_2$  and  $\text{O}_2\text{-N}_2$ , *Journal of Computational Chemistry* 32 (2) (2010) 279–290. doi:10.1002/jcc.21619.
- [9] M. Hausmann, U. Platt, Spectroscopic measurement of bromine oxide and ozone in the high arctic during polar sunrise experiment 1992, *Journal of Geophysical Research* 99 (D12) (1994) 25399. doi:10.1029/94jd01314.
- [10] V. Distelrath, U. Boesl, Mass selective gas phase study of  $\text{ClO}$ ,  $\text{OCIO}$ ,  $\text{ClOO}$  and  $\text{ClAr}$  by anion-zeke-photoelectron spectroscopy, *Faraday Discussions* 115 (2000) 161–174. doi:10.1039/a909618c.
- [11] R. Wayne, *Chemistry of Atmospheres*, 3rd Edition, Oxford University Press, New York, 2000.
- [12] L. Gipson, Pluto wags its tail: New horizons discovers a cold, dense region of atmospheric ions behind pluto (July 2015). URL <http://www.nasa.gov/nh/pluto-wags-its-tail>
- [13] F. D. Stacey, The possible occurrence of negative nitrogen ions in the atmosphere, *Journal of Geophysical Research* 64 (8) (1959) 979–981. doi:10.1029/jz064i008p00979.
- [14] L. G. Christophorou, *Electron-molecule interactions and their applications*, Academic Press Inc., London, 1984.
- [15] K. M. L. Lapere, M. Kettner, P. D. Watson, A. J. McKinley, D. A. Wild, Halidenitrogen gas-phase clusters: Anion photoelectron spectroscopy and high level ab initio calculations, *The Journal of Physical Chemistry A* 119 (37) (2015) 9722–9728. doi:10.1021/acs.jpca.5b06348.
- [16] T. Matsubara, K. Hirao, Density functional study of the interaction of  $\text{H}_2$ ,  $\text{N}_2$ ,  $\text{O}_2$ ,  $\text{CO}$ , and  $\text{NO}$  diatomic molecules with  $\text{H}^-$ ,  $\text{Li}^-$ , and  $\text{F}^-$  anions. prediction of a new type of anion cluster, *The Journal of Physical Chemistry A* 107 (14) (2003) 2505–2515. doi:10.1021/jp021266q.
- [17] K. Hiraoka, M. Nasu, J. Katsuragawa, T. Sugiyama, E. W. Ignacio, S. Yamabe, How is the fluoride ion bound to  $\text{O}_2$ ,  $\text{N}_2$ , and  $\text{CO}$  molecules?, *The Journal of Physical Chemistry A* 102 (35) (1998) 6916–6920. doi:10.1021/jp9812637.
- [18] S. Grimme, Accurate description of van der waals complexes by density functional theory including empirical corrections, *Journal of Computational Chemistry* 25 (12) (2004) 1463–1473. doi:10.1002/jcc.20078.
- [19] O. Cheshnovsky, S. H. Yang, C. L. Pettiette, M. J. Craycraft, R. E. Smalley, Magnetic time-of-flight photoelectron spectrometer for mass-selected negative cluster ions, *Review of Scientific Instruments* 58 (11) (1987) 2131–2137. doi:10.1063/1.1139475.
- [20] W. C. Wiley, I. H. McLaren, Time of flight mass spectrometer with improved resolution, *Rev. Sci. Instrum.* 26 (1955) 1150–1157. doi:10.1063/1.1715212.

- [21] A. Karton, M. Kettner, D. Wild, Sneaking up on the criegee intermediate from below: Predicted photoelectron spectrum of the  $\text{CH}_2\text{OO}^-$  anion and W3-F12 electron affinity of  $\text{CH}_2\text{OO}$ , *Chemical Physics Letters* 585 (2013) 15–20. doi:10.1016/j.cplett.2013.08.075.
- [22] K. Lapere, R. LaMacchia, L. Quak, A. McKinley, D. Wild, Anion photoelectron spectroscopy and ab initio calculations of the gas phase chloridocarbon monoxide complex:  $\text{Cl}\cdots\text{CO}$ , *Chemical Physics Letters* 504 (1-3) (2011) 13–19. doi:10.1016/j.cplett.2011.01.034.
- [23] K. Lapere, Anion photoelectron spectroscopy of halide complexes and clusters, Ph.D. thesis, University of Western Australia: School of Chemistry and Biochemistry (2014).
- [24] M. J. Frisch, G. W. Trucks, H. B. Schlegel, G. E. Scuseria, M. A. Robb, J. R. Cheeseman, G. Scalmani, V. Barone, B. Mennucci, G. A. Petersson, H. Nakatsuji, M. Caricato, X. Li, H. P. Hratchian, J. Izmaylov, A. F.; Bloino, G. Zheng, J. L. Sonnenberg, M. Hada, M. Ehara, K. Toyota, R. Fukuda, J. Hasegawa, M. Ishida, T. Nakajima, Y. Honda, O. Kitao, H. Nakai, T. Vreven, J. Montgomery, J. A., J. E. Peralta, F. Ogliaro, M. Bearpark, J. J. Heyd, E. Brothers, K. N. Kudin, V. N. Staroverov, R. Kobayashi, J. Normand, K. Raghavachari, A. Rendell, J. C. Burant, S. S. Iyengar, J. Tomasi, M. Cossi, N. Rega, M. J. Millam, M. Klene, J. E. Knox, J. B. Cross, V. Bakken, C. Adamo, J. Jaramillo, R. Gomperts, R. E. Stratmann, O. Yazyev, A. J. Austin, R. Cammi, C. Pomelli, J. W. Ochterski, R. L. Martin, K. Morokuma, V. G. Zakrzewski, G. A. Voth, P. Salvador, J. J. Dannenberg, S. Dapprich, A. D. Daniels, J. P. Farkas, J. B. Foresman, J. V. Ortiz, J. Cioslowski, D. J. Fox, Gaussian 09 revision d.01, gaussian Inc. Wallingford CT 2009.
- [25] T. H. Dunning, Gaussian basis sets for use in correlated molecular calculations. i. the atoms boron through neon and hydrogen, *The Journal of Chemical Physics* 90 (2) (1989) 1007–1023. doi:10.1063/1.456153.
- [26] T. H. Dunning, K. A. Peterson, A. K. Wilson, Gaussian basis sets for use in correlated molecular calculations. x. the atoms aluminum through argon revisited, *The Journal of Chemical Physics* 114 (21) (2001) 9244–9253. doi:10.1063/1.1367373.
- [27] G. Maroulis, A. J. Thakkar, Multipole moments, polarizabilities, and hyperpolarizabilities for  $\text{N}_2$  from fourth-order many-body perturbation theory calculations, *J. Chem. Phys.* 88 (12) (1988) 7623–7632. doi:10.1063/1.454327.
- [28] D. Jayatilaka, D. J. Grimwood, Tonto: A fortran based object-oriented system for quantum chemistry and crystallography, *Computational Science ICCS 2003* (2003) 142–151.
- [29] K. M. Lapere, R. J. LaMacchia, L. H. Quak, M. Kettner, S. G. Dale, A. J. McKinley, D. A. Wild, The bromide-carbon monoxide gas phase complex: Anion photoelectron spectroscopy and ab initio calculations, *Australian Journal of Chemistry* 65 (5) (2012) 457–462. doi:10.1071/ch12007.
- [30] L. J. Radziemski, V. Kaufman, Wavelengths, energy levels, and analysis of neutral atomic chlorine ( $\text{Cl I}$ ), *J. Opt. Soc. Am.* 59 (4) (1969) 424–443. doi:10.1364/josa.59.000424.